

## Enhanced ionization of the H<sub>2</sub> molecule driven by intense ultrashort laser pulses

E. Dehghanian and A. D. Bandrauk

*Département de Chimie, Université de Sherbrooke, Sherbrooke, Québec, Canada J1K 2R1*

G. Lagmago Kamta

*Department of Medical Physics, The Ottawa Hospital Cancer Centre, Ottawa, Ontario, Canada K1H 8L6*

(Received 8 April 2010; published 24 June 2010)

We report correlated two-electron *ab initio* calculations for the hydrogen molecule H<sub>2</sub> in interaction with intense ultrashort laser pulses, via a solution of the full three-dimensional time-dependent Schrödinger equation. Our results for ionization and excitation probabilities (at 800 and 400 nm) as a function of internuclear distance  $R$  show strong evidence of enhanced ionization, in both single and double ionization, as well as enhanced excitation, in single and double excitation, as the internuclear distance  $R$  increases from the equilibrium value  $R_e$ . The enhancement of all these molecular processes exhibits a maximum at a critical distance  $R_c$ , which can be predicted from simple electrostatic and recollision models.

DOI: 10.1103/PhysRevA.81.061403

PACS number(s): 33.80.Rv, 33.80.Wz, 33.80.Eh, 42.50.Hz

As the internuclear distance of molecular systems driven by intense laser fields increases beyond the equilibrium internuclear distance  $R_e$ , the ionization rate increases significantly, reaching a peak at some critical internuclear separation  $R_c$ ; it then decreases to atomic ionization rates for  $R$  values beyond  $R_c$  in symmetric molecules. This phenomenon, known as charge-resonance-enhanced ionization (CREI) for symmetric molecules, has been predicted by theoretical studies [1,2] and confirmed by various experiments [3]. The theoretical investigation of CREI for symmetric molecular systems driven by intense laser pulses [1,2] has been extended to nonsymmetric [4] molecules with only one active electron and is generally known as enhanced ionization (EI). The first papers [1,2] arrived at a theoretical expression for the CREI critical distance  $R_c$  for one electron which has been generalized to one-dimensional (1D) models of symmetric two-electron systems such as H<sub>2</sub> [5,6], H<sub>3</sub><sup>+</sup> [7] and H<sub>4</sub><sup>2+</sup> [5]. Three-dimensional Born-Oppenheimer simulations for H<sub>2</sub> [8,9] have addressed the question of electron correlation in ionization, and experiment has confirmed recollision dynamics in D<sub>2</sub> and H<sub>2</sub> [10]. Recently, a 2D two-electron model has confirmed the importance of electron correlation in high-order harmonic generation [11]. A previous 1D comparison of single and double ionization in H<sub>2</sub> as a function of  $R$  supported recollision [12] as an important mechanism [13]. The role of intermediate ionic states H<sup>+</sup>H<sup>-</sup> [14] as precursors to EI was emphasized in [5,7,8,15].

In this work, we solve the full-dimensional time-dependent Schrödinger equation (TDSE) for the H<sub>2</sub> molecule with two active electrons driven by an intense laser pulse. Spheroidal coordinates are used with electron-electron correlations included, and the TDSE is expanded in a basis of Laguerre and Legendre polynomials as for H<sub>2</sub><sup>+</sup> [4]. Results for the H<sub>2</sub> molecule show that processes leading to the breakup of the molecule, that is, single and double ionization and single and double excitation, are all strongly enhanced as the internuclear distance increases. We find that all these processes are maximum at nearly the same critical internuclear distance  $R_c$  and then they decrease for internuclear distances larger than  $R_c$ . A simple theoretical expression is derived for  $R_c$  in a similar formalism as for 1D models [5,7] and the 3D formalism [8]. The TDSE for a

two-electron diatomic molecular system with fixed nuclei is

$$i \frac{\partial}{\partial t} \Psi(\mathbf{r}_1, \mathbf{r}_2, t) = [H + D(t)] \Psi(\mathbf{r}_1, \mathbf{r}_2, t), \quad (1)$$

where  $\Psi(\mathbf{r}_1, \mathbf{r}_2, t)$  is the electronic wave function,  $H = K_e + V_N + U_c$  is the field-free electronic Hamiltonian,  $K_e = \mathbf{p}_1^2/2 + \mathbf{p}_2^2/2$  is the kinetic energy of the two electrons, and  $\mathbf{p}_j = -i\nabla_j$  is the momentum of electron  $j$ .  $V_N = -Z_a(1/r_{1a} + 1/r_{2a}) - Z_b(1/r_{1b} + 1/r_{2b})$  is the Coulomb attraction between the nuclei  $a$  and  $b$  and the two electrons, where  $r_{ja} = |\mathbf{r}_j + \mathbf{R}/2|$  ( $r_{jb} = |\mathbf{r}_j - \mathbf{R}/2|$ ) denotes the distance between the nucleus  $a$  (nucleus  $b$ ) and electron  $j$  ( $j = 1, 2$ ).  $\mathbf{R}$  is the internuclear vector and  $Z_a$  and  $Z_b$  are the nuclear charges.  $\mathbf{r}_j$  is the electron coordinate relative to the geometric center of the molecule.  $U_c = 1/r_{12}$  is the electron-electron repulsion potential, where  $r_{12} = |\mathbf{r}_1 - \mathbf{r}_2|$  denotes the electron-electron distance.  $D(t)$  is the Hamiltonian for the interaction of the molecule with the laser, which is given by  $D(t) = \mathbf{E}(t) \cdot (\mathbf{r}_1 + \mathbf{r}_2)$  in the length gauge and by  $D(t) = \mathbf{A}(t) \cdot (\mathbf{p}_1 + \mathbf{p}_2)$  in the velocity gauge. However except in Figs. 1(a) and 2(a), only the velocity gauge is used in this work because of its rapid convergence [4]. The vector potential of the laser field is  $\mathbf{A}(t) = A_0 f(t) \sin(\omega_0 t) \mathbf{e}_z$ , where  $A_0$  is the maximum amplitude,  $f(t)$  is the cosine square pulse envelope,  $\omega_0$  is the laser frequency, and  $\mathbf{e}_z$  is the unit vector along the laser polarization axis  $z$ , which is assumed to be parallel to the internuclear axis. The electric field of the laser pulse is determined from  $\mathbf{A}(t)$  as  $\mathbf{E}(t) = -(\partial/\partial t)\mathbf{A}(t)$ , so the total field area is zero. Atomic units (a.u.) are used throughout this work.

In order to solve the TDSE (1), we use prolate spheroidal coordinates [4]  $(\xi, \eta, \phi)$ , where  $\xi = (r_1 + r_2)/R$ ,  $\eta = (r_1 - r_2)/R$ , and  $\phi$  is the azimuthal angle. The time-dependent wave function is expanded in a basis as

$$\begin{aligned} \Psi(\mathbf{r}_1, \mathbf{r}_2, t) = & \sum_{m, \mu_1, \mu_2}^{v_1, v_2} \psi_{m, \mu_1, \mu_2}^{v_1, v_2}(t) [1 + \varepsilon_\phi \varepsilon_p P_{12}] \\ & \times U_{v_1}^m(\xi_1) V_{\mu_1}^m(\eta_1) U_{v_2}^m(\xi_2) V_{\mu_2}^m(\eta_2) \\ & \times (-1)^m \frac{e^{im(\phi_1 - \phi_2)} + \varepsilon_\phi e^{-im(\phi_1 - \phi_2)}}{2\pi}, \quad (2) \end{aligned}$$

where  $\psi_{m,\mu_1,\mu_2}^{\nu_1,\nu_2}(t)$  are time-dependent coefficients.  $[1 + \varepsilon_\phi \varepsilon_p P_{12}]$  is an antisymmetrization operator that projects onto singlet states in accordance with the Pauli exclusion principle ( $\varepsilon_p = +1$  for singlet states and  $\varepsilon_\phi = +1$  for  $\Sigma^+$  states).  $P_{12}$  is an operator that exchanges the parameters  $(\mu_1, \nu_1)$  and  $(\mu_2, \nu_2)$  in order to ensure the indistinguishability of the two electrons. Equation (2) accounts for the fact that we are only dealing with  $\Sigma$  states, for which the projection of the total angular momentum  $M$  of the electron along the  $z$  axis is zero.  $U_v^m(\xi)$  and  $V_\mu^m(\eta)$  are basis functions expressed in terms of Laguerre  $L_{v-|m|}^{2|m|}$  and Legendre polynomials  $P_\mu^m(\eta)$  [4] as  $U_v^m(\xi) = N_v^m e^{-\alpha(\xi-1)} (\xi^2 - 1)^{|m|/2} L_{v-|m|}^{2|m|} [2\alpha(\xi - 1)]$  and  $V_\mu^m(\eta) = M_\mu^m P_\mu^m(\eta)$ . The basis indices take the values  $m = 0, \pm 1, \pm 2, \dots$ ;  $\mu = |m|, |m| + 1, |m| + 2, |m| + \mu_{\max}$ , and  $\nu = |m|, |m| + 1, |m| + 2, |m| + \nu_{\max}$ . The electron-electron correlation is included in our calculation by means of the Neumann expansion:

$$\frac{1}{r_{12}} = \frac{4}{R} \sum_{l=0}^{\infty} \sum_{n=-l}^{+l} S_l^n P_l^{|n|}(\xi_{<}) Q_l^{|n|}(\xi_{>}) \times P_l^{|n|}(\eta_1) P_l^{|n|}(\eta_2) e^{in(\phi_1 - \phi_2)}, \quad (3)$$

where  $S_l^n = (-1)^n [(2l+1)/2]! [(l-|n|)!/(l+|n|)!]$ , and  $\xi_{<}$  and  $\xi_{>}$  are the lesser and the greater values of  $\xi_1$  and  $\xi_2$ , respectively.  $P_l^n$  and  $Q_l^n$  are associated Legendre functions of the first and second kind, respectively [4]. Projection of the stationary Schrödinger equation  $H\Psi = E\Psi$  and the TDSE onto the basis (2) leads, respectively, to the field-free eigenvalue equation  $\mathbf{H}\Psi = \mathbf{E}\mathbf{S}\Psi$  and to the system of first-order differential equations

$$i \frac{\partial}{\partial t} \mathbf{S}\Psi(t) = [\mathbf{H} + g(t)\mathbf{D}]\Psi(t), \quad (4)$$

where  $\Psi$  is the vector representation of the wave function, and  $g(t) = -iA(t)$  in the velocity gauge and  $g(t) = E(t)$  in the length gauge.  $\mathbf{S}$ ,  $\mathbf{H}$ , and  $\mathbf{D}$  are the overlap, exact Hamiltonian, and dipole matrix, respectively. The field-free solution of the eigenvalue equation  $\mathbf{H}\Psi = \mathbf{E}\mathbf{S}\Psi$  yields eigenvalues and eigenfunctions of  $H_2$  for each  $R$ ; in particular, the initial state wave function for time propagation of the TDSE. As discussed before [4], we further project the TDSE (4) onto the eigenstate representation, where it becomes  $i(\partial/\partial t)\Phi(t) = [\mathbf{h} + g(t)\mathbf{W}]\Phi(t)$ . In this equation  $\mathbf{h}$  is a diagonal matrix containing eigenvalues of the field-free molecular Hamiltonian  $\mathbf{H}$ , and  $\mathbf{W}$  is the dipole matrix in the eigenstate basis. In this representation, the wave function  $\Phi(T)$  at the end of the laser pulse (at time  $t = T$ ) is a superposition of probability amplitudes for finding the system in eigenstates of the field-free Hamiltonian, that is,  $\Phi(T) = \sum_i C_i(T)\Phi_i$ , where  $\Phi_i$  is the electronic eigenstate of energy  $E_i$  and  $C_i(T)$  is its probability amplitude. Single- ( $P_{\text{SI}}$ ) and double- ( $P_{\text{DI}}$ ) ionization probabilities are obtained by projecting the final two-electron wave function  $\Psi(\mathbf{r}_1, \mathbf{r}_2, t)$  as follows [13,16,17]:

$$P_{\text{SI}} = \sum_{m_1, E_1} \sum_{m_2, E_2} \left| \langle \varphi_{E_1, E_2}^{m_1, m_2}(\mathbf{r}_1, \mathbf{r}_2) | \Psi(\mathbf{r}_1, \mathbf{r}_2, T) \rangle \right|^2, \quad (5)$$

$$P_{\text{DI}} = \sum_{m_1, E_1} \sum_{m_2, E_2} \left| \langle \varphi_{E_1, E_2}^{m_1, m_2}(\mathbf{r}_1, \mathbf{r}_2) | \Psi(\mathbf{r}_1, \mathbf{r}_2, T) \rangle \right|^2, \quad (6)$$

where

$$\varphi_{E_1, E_2}^{m_1, m_2}(\mathbf{r}_1, \mathbf{r}_2) = N [\varphi_{E_1}^{m_1}(\mathbf{r}_1) \varphi_{E_2}^{m_2}(\mathbf{r}_2) + \varepsilon_p \varphi_{E_1}^{m_2}(\mathbf{r}_2) \varphi_{E_2}^{m_1}(\mathbf{r}_1)] \quad (7)$$

is an antisymmetrized product of a bound  $[\varphi_{E_1}^{m_1}(\mathbf{r}_1)]$  and a continuum orbital  $[\varphi_{E_2}^{m_2}(\mathbf{r}_2)]$  of  $H_2^+$ , where  $m_1$  and  $m_2$  are their angular momentum projections and  $E_1$  and  $E_2$  are their energies. Similarly,

$$\varphi_{E_1, E_2}^{m_1, m_2}(\mathbf{r}_1, \mathbf{r}_2) = N [\varphi_{E_1}^{m_1}(\mathbf{r}_1) \varphi_{E_2}^{m_2}(\mathbf{r}_2) + \varepsilon_p \varphi_{E_1}^{m_2}(\mathbf{r}_2) \varphi_{E_2}^{m_1}(\mathbf{r}_1)] \quad (8)$$

is an antisymmetrized products of two orbitals of  $H_2^+$  in which both electrons are in the continuum. The wave function (7) describes a two-electron state where one electron is still bound and the other is in a continuum state, whereas Eq. (8) represents a state in which both electrons are in a continuum. Therefore the single-ionization probability in Eq. (5) is obtained as a sum of probability amplitudes for all combinations in which one electron is in a bound state and the other is in a continuum, and similarly for double ionization in Eq. (6) as a sum over all configurations where both electrons are in a continuum. Given that Eqs. (7) and (8) are *uncorrelated*, obtaining single and double ionization in this way amounts to neglecting correlation in the final state. The above projection method for the extraction of single and double ionization yields satisfactory and practical results [16–18].

In order to assess further information on the breakup of the molecule, we also compute the following quantities from the total two-electron wave function  $\Psi(\mathbf{r}_1, \mathbf{r}_2, t)$ , Eq. (2), at the end of the laser pulse: The total ionization probability  $P_{\text{TI}}$  is defined as the probability of finding the molecule in eigenstates of  $H_2$  with energies larger than the single-ionization threshold  $I_p$ , the sum of probabilities for single and double ionization and double excitation, and the total excitation probability  $P_{\text{TE}}$  is the sum of probability amplitudes for finding the electron in excited states below the double-ionization state, that is,

$$P_{\text{TI}} = 1 - \sum_{E_i < I_p} |C_i(T)|^2, \quad (9)$$

$$P_{\text{TE}} = \sum_{E_i < 0} |C_i(T)|^2 - |C_1(T)|^2.$$

$|C_i(T)|^2$  is the probability of finding the system at the end of the laser pulse in the electronic eigenstate of energy  $E_i$ . The single-excitation probability  $P_{\text{SE}}$ , which is the sum of probability amplitudes for finding the electron in excited states below the single-ionization state, becomes then

$$P_{\text{SE}} = \sum_{E_i < I_p} |C_i(T)|^2 - |C_1(T)|^2, \quad (10)$$

$$P_{\text{DE}} = P_{\text{TI}} - P_{\text{SI}} - P_{\text{DI}},$$

and the double-excitation probability is defined as  $P_{\text{DE}}$ . Our results are summarized in Figs. 1 and 2 for  $\omega = 0.114$  and  $0.057$  a.u. for various laser peak intensities. The convergence of results is assessed by increasing the basis size until the results become relatively unchanged with further increase of the basis size. The results obtained from both length and velocity gauges agree [Figs. 1(a)

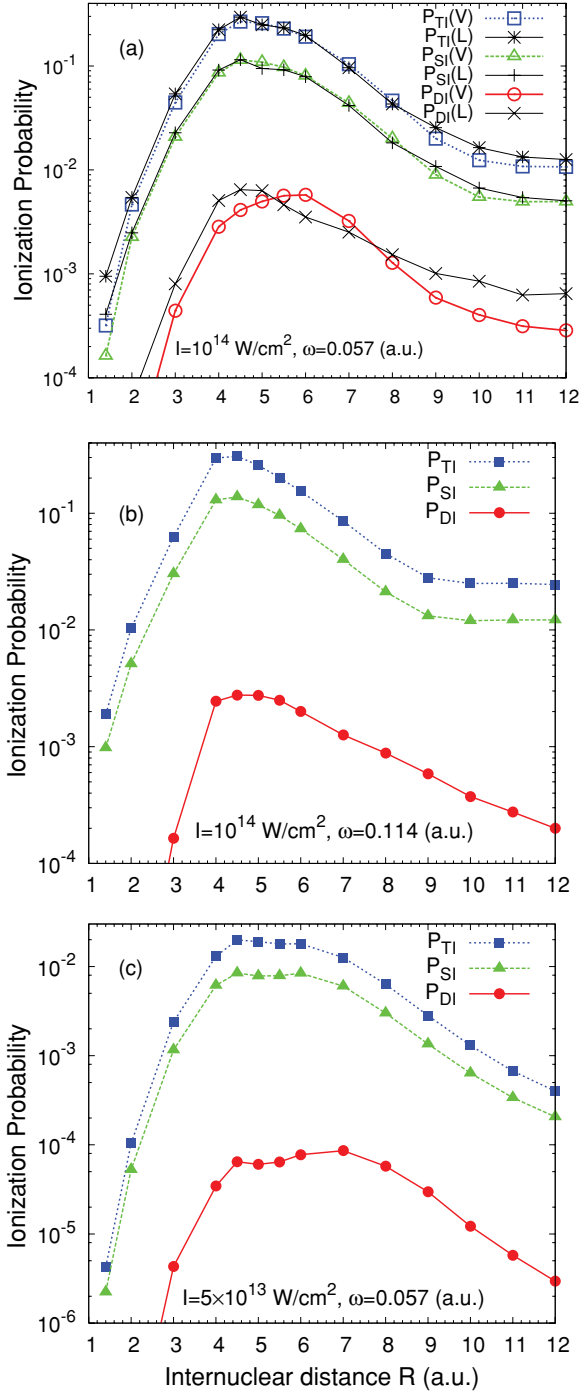


FIG. 1. (Color online) Total ( $P_{TI}$ ), single- ( $P_{SI}$ ), and double- ( $P_{DI}$ ) ionization probabilities of H<sub>2</sub> by a four-cycle laser pulse for two different frequencies and intensities (V, velocity gauge, and L, length gauge): (a)  $I = 10^{14}$  W/cm<sup>2</sup>,  $\omega = 0.057$  a.u. (b)  $I = 10^{14}$  W/cm<sup>2</sup>,  $\omega = 0.114$  a.u. (c)  $I = 5 \times 10^{13}$  W/cm<sup>2</sup>,  $\omega = 0.057$  a.u.

and 2(a)] and this confirms the accuracy of our numerical procedure.

We use laser pulses of intensities  $10^{13} \leq I \leq 10^{14}$  W/cm<sup>2</sup> with a total pulse duration of four cycles. We have also performed the calculation for six cycles and found that both ionization and excitation maxima are independent of the pulse duration. The total  $P_{TI}$ , single-  $P_{SI}$ , and double-ionization  $P_{DI}$  probabilities of H<sub>2</sub> versus the internuclear distance  $R$  are

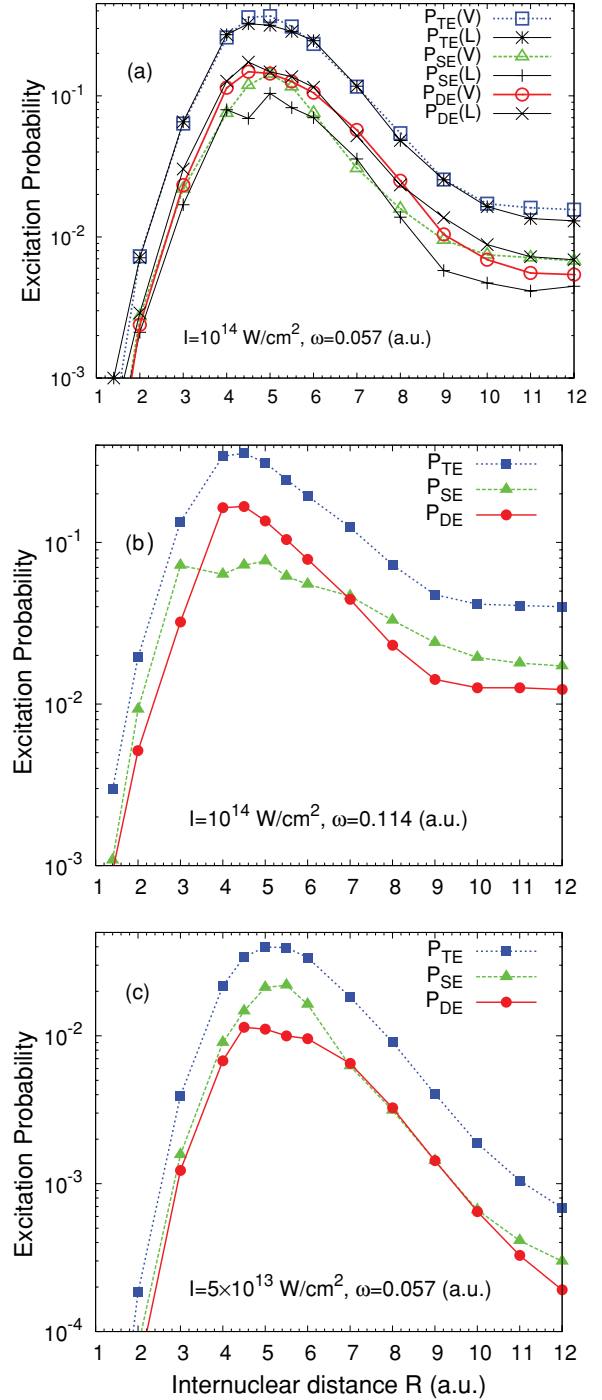


FIG. 2. (Color online) Total ( $P_{TE}$ ), single- ( $P_{SE}$ ), and double- ( $P_{DE}$ ) excitation probabilities of H<sub>2</sub> by a four-cycle laser pulse for two different frequencies and intensities (V, velocity gauge, and L, length gauge): (a)  $I = 10^{14}$  W/cm<sup>2</sup>,  $\omega = 0.057$  a.u. (b)  $I = 10^{14}$  W/cm<sup>2</sup>,  $\omega = 0.114$  a.u. (c)  $I = 5 \times 10^{13}$  W/cm<sup>2</sup>,  $\omega = 0.057$  a.u.

plotted in Figs. 1(a) and 1(b), respectively, for the frequencies  $\omega = 0.057$  and  $0.114$  a.u. with the laser peak intensity  $I = 10^{14}$  W/cm<sup>2</sup>. In both cases the total, single-, and double-ionization probabilities increase as we go to larger internuclear distances, and at some critical point  $R_c \simeq 4.5\text{--}5$  a.u. a maximum is reached (at  $\omega = 0.057$  a.u.,  $R_c = 6$  a.u. for double ionization); the probabilities then decrease at larger internuclear distances. The EI behavior and critical internuclear distance

$R_c$  for lower laser intensity  $I = 5 \times 10^{13}$  W/cm<sup>2</sup> and  $\omega = 0.057$  a.u. [Fig. 1(c)] is almost the same as for  $I = 10^{14}$  W/cm<sup>2</sup> in Fig. 1(a). The excitation probabilities in Fig. 2 show features similar to those of the ionization probabilities in Figs. 1(a)–1(c): at higher intensity  $I = 10^{14}$  W/cm<sup>2</sup>, total and single excitation are enhanced at the same critical distance ( $R_c = 4.5$  a.u.) as total and single ionization for both frequencies  $\omega = 0.057$  a.u. and 0.114 a.u., but double-excitation probabilities are enhanced at  $R = 5$  a.u. At lower intensity  $I = 5 \times 10^{13}$  W/cm<sup>2</sup>,  $\omega = 0.057$  a.u., total, single, and double excitations are enhanced at  $R_c \simeq 5$  a.u., with a shoulder at  $R = 7$  a.u. for the single excitation. The most intriguing aspect of the results in Figs. 1 and 2 is the parallel behavior as a function of  $R$  of all ionization and excitation process probabilities: a common maximum at a critical distance  $R_c$  and parallel probability distributions around  $R_c$  for two different intensities and frequencies. The value of  $R_c \simeq 5$  a.u. for EI for the single-ionization probability  $P_{SI}$  (5) can be estimated from an electrostatic model based on the creation of the precursor ionic state  $H^+H^-$  [5,7,8,15] at the laser peak intensities. The energy difference  $\Delta E$  between this ionic state  $H^+H^-$  and the covalent (neutral) ground state in a field strength  $\varepsilon$  is  $\Delta E = E(HH) - E(H^+H^-) = \Delta I_p - 1/R - \varepsilon R$ , where  $\Delta I_p = I_p(H) - I_p(H^-) \simeq 0.47$  a.u., the ionization potential energy difference.  $-1/R$  is the

Coulomb attraction between  $H^+$  and  $H^-$  and  $\varepsilon R$  is the electrostatic potential energy of  $H^-$  in the field  $\varepsilon$  at distance  $R$ . Charge transfer from the covalent (neutral) HH state to the ionic state  $H^+H^-$  and its subsequent ionization will occur at  $\Delta E = 0$ . Thus at intensity  $I = 10^{14}$  W/cm<sup>2</sup>,  $\varepsilon = 0.053$  a.u., one obtains readily from the above equation  $R_c = 5$  a.u., in good agreement with Figs. 1 and 2. The second-ionization probability  $P_{DI}$  should reach its maximum at  $R_c \simeq 4/I_p(H) \simeq 7-8$  a.u. as in  $H_2^+$  [1]. Figures 1 and 2 show that  $P_{DI}$  has the same  $R_c$  as the single ionization  $P_{SI}$  from  $H^+H^-$ . This can be explained by the recollision model, where second ionization occurs following recollision of the first ionized electron with the parent ion in atoms [12] and molecules [13]. Thus, since the first ionization  $P_{SI}$  occurs at  $R_c \simeq 5$  a.u., the second ionization  $P_{DI}$  and excitations  $P_{SE}$  and  $P_{DE}$  and possibly shakeup processes [19] are induced by this first process, so all occur at the same  $R_c$ , a signature of recollision dynamics. Only  $\Sigma_g^+$  and  $\Sigma_u^+$  doubly excited states can be populated with linear parallel polarization. Such states are generally coupled by radiative transition moments, which diverge as  $R/\sqrt{2}$  [1]. Increasing intensities and internuclear distance will therefore increase the population of such states, as shown in Fig. 2. Such doubly excited states have been studied in [20] and could be a mechanism for the unusual crossing of populations calculated in Fig. 2.

- 
- [1] T. Zuo and A. D. Bandrauk, *Phys. Rev. A* **52**, R2511 (1995).  
 [2] T. Seideman, M. Yu. Ivanov, and P. B. Corkum, *Phys. Rev. Lett.* **75**, 2819 (1995).  
 [3] C. Cornaggia, in *Progress in Ultrafast Intense Laser Science*, edited by K. Yamanouchi *et al.* (Springer, Tokyo, 2010), Vol. VI (to appear).  
 [4] G. L. Kamta and A. D. Bandrauk, *Phys. Rev. Lett.* **94**, 203003 (2005); *Phys. Rev. A* **76**, 053409 (2007); **71**, 053407 (2005).  
 [5] H. Yu, T. Zuo, and A. D. Bandrauk, *Phys. Rev. A* **54**, 3290 (1996); *J. Phys. B* **31**, 1533 (1998).  
 [6] I. Kawata, H. Kono, Y. Fujimura, and A. D. Bandrauk, *Phys. Rev. A* **62**, 031401(R) (2000).  
 [7] I. Kawata, H. Kono, and A. D. Bandrauk, *Phys. Rev. A* **64**, 043411 (2001).  
 [8] K. Harumiya, H. Kono, Y. Fujimura, I. Kawata, and A. D. Bandrauk, *Phys. Rev. A* **66**, 043403 (2002).  
 [9] A. Saenz, *Phys. Rev. A* **66**, 063407 (2002).  
 [10] A. S. Alnaser, T. Osipov, E. P. Benis, A. Wech, B. Shan, C. L. Cocke, X. M. Tong, and C. D. Lin, *Phys. Rev. Lett.* **91**, 163002 (2003).  
 [11] S. Sukiasyan, C. McDonald, C. Destefani, M. Y. Ivanov, and T. Brabec, *Phys. Rev. Lett.* **102**, 223002 (2009).  
 [12] P. B. Corkum, *Phys. Rev. Lett.* **71**, 1994 (1993).  
 [13] A. D. Bandrauk and H. Z. Lu, *Phys. Rev. A* **72**, 023408 (2005).  
 [14] G. Corongiu and E. Clementi, *J. Phys. Chem. A* **113**, 14791 (2009).  
 [15] S. Saugout, C. Cornaggia, A. Suzor-Weiner, and E. Charron, *Phys. Rev. Lett.* **98**, 253003 (2007).  
 [16] E. Fomouo, G. L. Kamta, G. Edah, and B. Piraux, *Phys. Rev. A* **74**, 063409 (2006).  
 [17] R. Grobe and J. H. Eberly, *Phys. Rev. A* **48**, 4664 (1993).  
 [18] J. Colgan, M. S. Pindzola, and F. Robicieux, *J. Phys. B* **34**, L457 (2001); **41**, 121002 (2008).  
 [19] I. V. Litvinyuk, F. Légaré, P. W. Dooley, D. M. Villeneuve, P. B. Corkum, J. Zanghellini, A. Pegarkov, C. Fabian, and T. Brabec, *Phys. Rev. Lett.* **94**, 033003 (2005).  
 [20] I. Sánchez and F. Martín, *J. Chem. Phys.* **106**, 7720 (1997).